

Continuous-wave-controlled steering of spatial solitons

Yannis Kominis and Kyriakos Hizanidis

Department of Electrical and Computer Engineering, National Technical University of Athens, 9 Iroon Polytechniou, 157 73 Athens, Greece

Received March 12, 2003; revised manuscript received August 6, 2003; accepted August 12, 2003

Spatial-soliton interactions with continuous waves (cw's) are studied, with numerical simulations as well as a quasi-particle perturbation method, and the critical dependency of their features on the parameters of the cw is shown. The intentional mixing of appropriately launched cw's with spatial solitons is proposed as a technique for the design and implementation of all-optical, dynamically reconfigurable devices. © 2004 Optical Society of America

OCIS codes: 190.5530, 190.4360, 230.1150, 190.4420.

1. INTRODUCTION

Spatial solitons are robust, self-guided light beams described by solutions of the nonlinear Schrödinger equation (NLS) arising as a result of the balance between spatial diffraction and the self-focusing effects of a Kerr-type nonlinearity in a slab waveguide. These remarkable beams have been observed in a variety of materials such as glass, liquids, gases, semiconductors, and thin-film structures filled with nematic liquid crystals,¹⁻³ and under the presence of various non-Kerr nonlinearities, such as quadratic nonlinearities,⁴ as well as in photorefractive materials.⁵⁻⁷ The unique properties of spatial solitons make them ideal for all-optical, ultrafast routing and switching devices with great potential for applications in optical telecommunications. Signal beams can be easily controlled and switched by passing through such modules in an all-optical network. On the other hand, of particular interest is the concept of "light guiding light," which can be described as the phenomenon of a strong pump beam causing a material to act as a linear waveguide with a sech-squared-type refractive-index profile through the intensity dependency of the refractive index. Both bright and dark solitons can be used in order to form such soliton-induced waveguides capable of guiding a weaker probe (signal) beam of the same or different wavelength.⁸ According to this concept, multiple-port linear devices have been proposed for reconfigurable directional coupling, utilizing N -soliton collisions.^{9,10}

However, the remarkable stability of spatial solitons in planar (one-dimensional) geometries, which is a prerequisite for the aforementioned applications, does not persist in the case of beam propagation in bulk Kerr media. Solitons of the two-dimensional NLS equation are unstable for the case of Kerr-type nonlinearity. Namely, for focusing Kerr media, for instance, the field amplitude of the beam increases to infinity, and its width decreases to zero, resulting in beam collapse after a finite propagation distance.¹¹ Also, beam interaction with a weak probe beam is shown to result in beam splitting both in planar and bulk nonlinear media.¹²

In this work, the possibility of controlling and steering a spatial soliton in a planar geometry by mixing it with an intentionally launched continuous wave (cw), as shown in Fig. 1, is investigated: In Fig. 1(a) and Fig. 1(b), the propagation of an unperturbed spatial soliton and of a cw-controlled one are respectively shown. Depending upon the characteristics of the cw beam, one may steer the spatial soliton to a chosen output port, as illustrated in Fig. 1(c). Interactions between solitons and cw's have been previously studied for temporal solitons and weak cw by utilization of the perturbed inverse-scattering method¹³ as well as for the case of a zero-frequency difference between the pulse and the cw.¹⁴ Spatial-soliton interactions with cw's are strongly dependent on certain parameters of both beam and cw, leading to promising potential for various applications of all-optical devices utilizing the features of this interaction. The results obtained in this work are of a universal nature, since the model used is applicable to both spatial and temporal solitons of the NLS equation. Many useful applications, such as frequency control, can also be considered for the temporal soliton case, leading to promising optical devices.

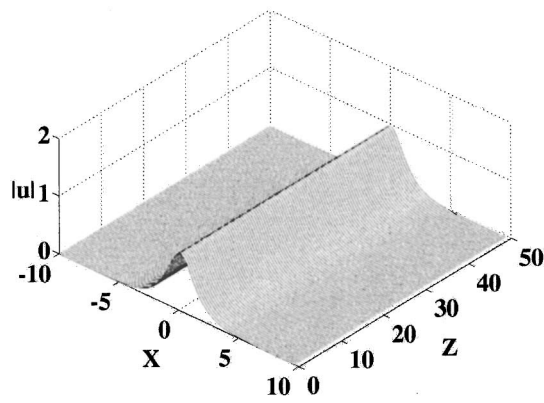
The present work is organized as follows: In Section 2, the model based on the quasi-particle approach is introduced. In Section 3, the main results are discussed and contrasted with direct simulations of the underlying NLS equation. Finally, the main features of cw-driven steering of spatial solitons are summarized in Section 4.

2. MODEL

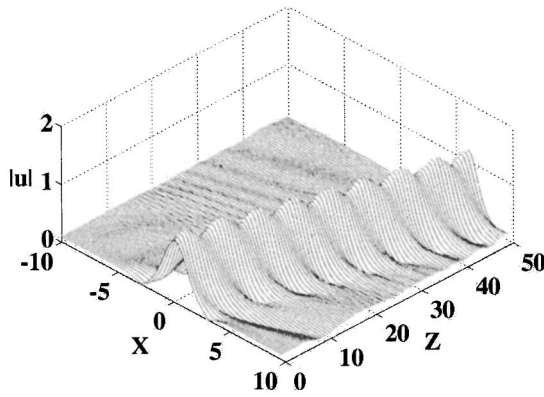
The NLS equation governing the propagation in a nonlinear medium has the normalized form

$$i \frac{\partial u}{\partial Z} + \frac{1}{2} \frac{\partial^2 u}{\partial X^2} + |u|^2 u = 0, \quad (1)$$

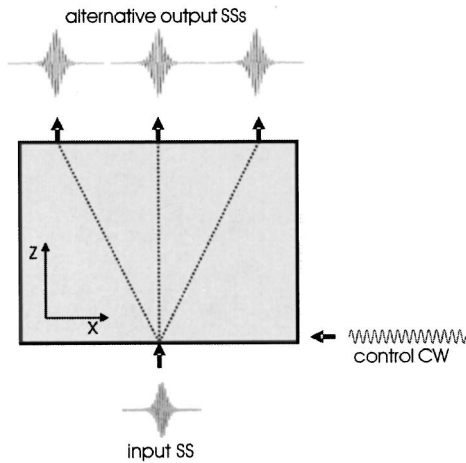
where the transverse distance, X , is normalized to the characteristic size of the beam a_0 , while the propagation distance, Z , is normalized to the corresponding diffraction distance $z_d = k_z a_0^2$, with k_z being the carrier longitudinal



(a)



(b)



(c)

Fig. 1. Propagation of a soliton beam (a) without injection of cw and (b) with injection of a cw having amplitude $a = 0.1$, transverse wave number $k_X = 1$, and initial phase $\phi = 0$, as obtained from direct numerical simulation of the NLS equation. (c) Illustration of the cw-controlled steering of an input spatial soliton (SS).

nal wave number. The normalized amplitude u is related to the amplitude of the electric field, E , through the relations

$$|u| = k_Z a_0 \sqrt{\frac{\epsilon_0 c n_2^I}{2}} |E| = \sqrt{\frac{k_Z z_d \epsilon_0 c n_2^I}{2}} |E|, \quad (2)$$

where n_2^I is the nonlinear refractive index (in units of m^2/W). The condition for beam self-trapping and spatial-soliton formation is evidently, on the basis of Eq. (1), $|u| \geq 1$; that is,

$$|E| \geq \frac{1}{k_Z a_0} \sqrt{\frac{2}{\epsilon_0 c n_2^I}}, \quad (3)$$

according to Eq. (2). The condition (3) reflects the need for highly nonlinear materials¹⁵ (high n_2^I) for practical applications (reasonably low threshold values for E): For example, for $\text{As}_{40}\text{Se}_{60}$ glass, the threshold value of the electric field intensity, in (V/m), is roughly in the range of $0.67 \times 10^9/a_0$ to $0.97 \times 10^9/a_0$ (with a_0 in μm) for carrier wavelengths in the range of 1.25 μm to 1.55 μm ¹⁶ and linear refractive index $n_0 \approx 1.45$. The respective range of the optical field intensity (in $\text{kW}/\mu\text{m}^2$) is in this case $0.86/a_0^2$ to $1.8/a_0^2$.

The NLS equation has the well-known bright-soliton solution $u_s(X, Z) = n \text{sech}[n(X + \kappa Z - X_0)] \exp(-i\kappa X + i\sigma)$, $\sigma = 1/2(n^2 - \kappa^2)Z$ representing a self-focused beam, with n and κ being the beam amplitude and transverse velocity (front tilt), respectively. On the other hand, the cw is a solution of the linearized NLS equation given by $u_{cw} = a \exp[-ik_X X - (1/2)k_X^2 Z + i\phi]$, where a , k_X , and ϕ denote the amplitude, the transverse wave number, and initial phase of the cw.

The evolution of the superposition of a bright soliton and a cw are now investigated, namely,

$$u = u_s + u_{cw}. \quad (4)$$

Substitution of Eq. (4) in the NLS equation (1) leads to a nonlinear term of the form $|u|^2 u = |u_s|^2 u_s + u_s^2 u_{cw}^* + 2|u_s|^2 u_{cw} + 2u_s |u_{cw}|^2 + u_{cw}^2 u_s^* + |u_{cw}|^2 u_{cw}$. After neglecting terms that are second and third order in $|u_{cw}|$ and using a separation of the aforementioned term on the basis of the degree of overlapping, we obtain the following set of equations:

$$i \frac{\partial u_s}{\partial Z} + \frac{1}{2} \frac{\partial^2 u_s}{\partial X^2} + |u_s|^2 u_s = R(u_s, u_{cw}), \quad (5)$$

$$i \frac{\partial u_{cw}}{\partial Z} + \frac{1}{2} \frac{\partial^2 u_{cw}}{\partial X^2} = 0, \quad (6)$$

where $R(u_s, u_{cw}) = u_s^2 u_{cw}^* + 2|u_s|^2 u_{cw}$ is the perturbation term modifying the soliton-beam propagation due to the presence of the cw, which fulfills the “linearized” NLS equation.

In order to study these interactions, a quasi-particle approach based on the perturbed-IST method¹⁷ is utilized. According to this method, the following equations govern the evolution of the soliton-beam parameters under propagation:

$$\frac{dn}{dZ} = \frac{1}{2} a \pi \operatorname{sech}\left(\frac{\omega \pi}{2}\right) n^2 (\omega^2 + 1) \sin(A), \quad (7)$$

$$\frac{d\kappa}{dZ} = -\frac{1}{2} a \pi \omega \operatorname{sech}\left(\frac{\omega \pi}{2}\right) n^2 (\omega^2 + 1) \sin(A), \quad (8)$$

$$\frac{dX_0}{dZ} = -\kappa - \frac{1}{2} a \pi \operatorname{sech}\left(\frac{\omega \pi}{2}\right) \left[-\frac{\pi}{2} \tanh\left(\frac{\omega \pi}{2}\right) (\omega^2 + 1) + 2\omega \right] \cos(A), \quad (9)$$

$$\frac{d\sigma}{dZ} = \frac{1}{2} (n^2 - \kappa^2) + X_0 \frac{d\kappa}{dZ} + \frac{1}{2} a \pi n \operatorname{sech}\left(\frac{\omega \pi}{2}\right) \times \left[\frac{\omega \pi}{2} \tanh\left(\frac{\omega \pi}{2}\right) (\omega^2 + 1) + 2 \right] \cos(A), \quad (10)$$

where $\omega = (k_X - \kappa)/n$ and $A = (k_X - \kappa)X_0 + 1/2k_X^2Z + \sigma - \phi$. A nonlinear oscillatory evolution depending strongly on the cw launch conditions is implied for the beam parameters according to these equations. As easily obtained by Eqs. (7) and (8), the quantity $|\omega|$ remains constant with respect to the propagation distance Z . This means that the variation of n and k is restricted on the straight lines $n = [n_0/(|\kappa_0 - k_X|)]|\kappa - k_X|$ with n_0, κ_0 denoting the initial values of the respective beam parameters. The position of the mean value of the parameter oscillations on these lines as well as their oscillation amplitude is determined by the amplitude a and the initial phase ϕ of the cw.

3. DISCUSSION

In the following, the initial beam transverse velocity κ as well as the initial position X_0 are considered zero for simplicity. The interaction between a spatial soliton having $n = 1$ and a cw with $k_X = \pm 1$ and $\phi = 0$ is shown in Figs. 2(a) and 2(b) for various cw amplitude values a : The contour plot of beam amplitude as obtained from direct numerical simulation of the NLS equation is shown in Fig. 2(a), while in Fig. 2(b) is shown the beam center X_0 as obtained by numerical integration of the parameter evolution equations. In Figs. 2(c) and 2(d), the beam amplitude oscillations as respectively obtained from direct numerical simulation of the NLS equation and the parameter evolution equations are contrasted for three cw amplitude values [$a = 0.05$ (dark solid curve), $a = 0.10$ (light semi-solid curve), and $a = 0.15$ (dotted curve)]. Additionally, the chirp oscillations as obtained from direct numerical simulation of the NLS equation are shown for these three cw amplitude values. The sign of the cw-induced transverse velocity of the beam is the opposite of the sign of transverse wave-number difference k_X , while its absolute value depends on the amplitude of the cw a . Apart from this change in transverse velocity, the beam is also affected in both amplitude and phase: The amplitude is no longer constant but undergoes oscillations as shown in Figs. 2(c) and 2(d). The periods of these oscillations decrease with cw amplitude while their magnitude

increases. Moreover, the mean value $\langle n \rangle$ of the amplitude also increases, resulting in an effective shift of the beam longitudinal wave number:

$$\Delta k_Z = (1/2)\langle n \rangle^2. \quad (11)$$

The phase of the beam is also distorted so that the transverse wave number is chirped along the X direction. Since the phase is not exactly quadratic in X , instead of using the usual parameter, we use an integral definition of the chirp as a weighted average of the second derivative of the phase¹⁸ $C = \operatorname{Im} \int_{-\infty}^{+\infty} u^2 u_X^{*2} / \int_{-\infty}^{+\infty} |u|^4$. The chirp oscillations shown in Fig. 2(e) have the same period with amplitude oscillations. Both amplitude and chirp oscillations do not depend on the sign of k_X .

The overall displacement of the center of the spatial solitary pulse, X_0 , as it propagates along z can be quantified by the parameter $\langle \kappa \rangle = -X_0(Z_{\max})/Z_{\max}$, that is, its mean transverse “velocity.” Direct numerical simulation of the NLS equation shows that, for a constant cw amplitude and phase difference, increasing of k_X (starting from zero) does not result in a monotonously increasing transverse velocity. This is shown in Figs. 3(a) and 3(b) for a beam interacting with a cw having $a = 0.1$ and $\phi = 0$. The transverse velocity increases until reaching a maximum value around $k_X \approx 1$ and then decreases until it becomes almost zero. In Fig. 3(c), the dependence of $\langle \kappa \rangle$ on k_X , as obtained by numerical integration of the parameter evolution equations, is shown for $a = 0.05, 0.10$, and 0.15 . For comparison, results from the direct numerical simulations in Figs. 3(a) and 3(b) are indicated by solid circles. This feature of the interaction is a result of a length-scale competition between the transverse wavelength of the cw and the beam characteristic size a_0 . When the cw wavelength is large compared with a_0 , soliton moves as an effective particle in the interaction-induced periodic potential, while in the opposite limit a “dressed” soliton emerges as a “renormalized” particle with almost zero velocity.¹⁹ Both the amplitude and spatial longitudinal frequency of the soliton amplitude and width oscillations depend also on the transverse wave number k_X of the cw, with the latter increasing with k_X .

The aforementioned interactions are also strongly dependent on the initial phase difference ϕ between the soliton beam and the cw at the launching point ($Z = 0$). Beam interaction with cw's having $k_X = 1$ and $a = 0.15$ are shown in Fig. 4(a) (direct numerical simulation of the NLS equation) for a variety of initial phase differences ϕ ($\phi = 0, \pi/3, \pi/2, 2\pi/3$, and π). When beam phase is initially in quadrature with the cw phase ($\phi = \pi/2$), the induced transverse velocity is quite small, while $\phi > \pi/2$ results in a transverse velocity of opposite sign. In Fig. 4(b), the beam mean transverse velocity $\langle \kappa \rangle$, as obtained by numerical integration of the parameter evolution equations, is plotted versus ϕ . Also, for comparison, results from the direct numerical simulations in Fig. 4(a) are indicated by solid circles.

4. CONCLUSION

In conclusion, spatial-soliton interactions with cw's have been numerically studied. It is shown that soliton beams change their transverse velocity as well as amplitude,

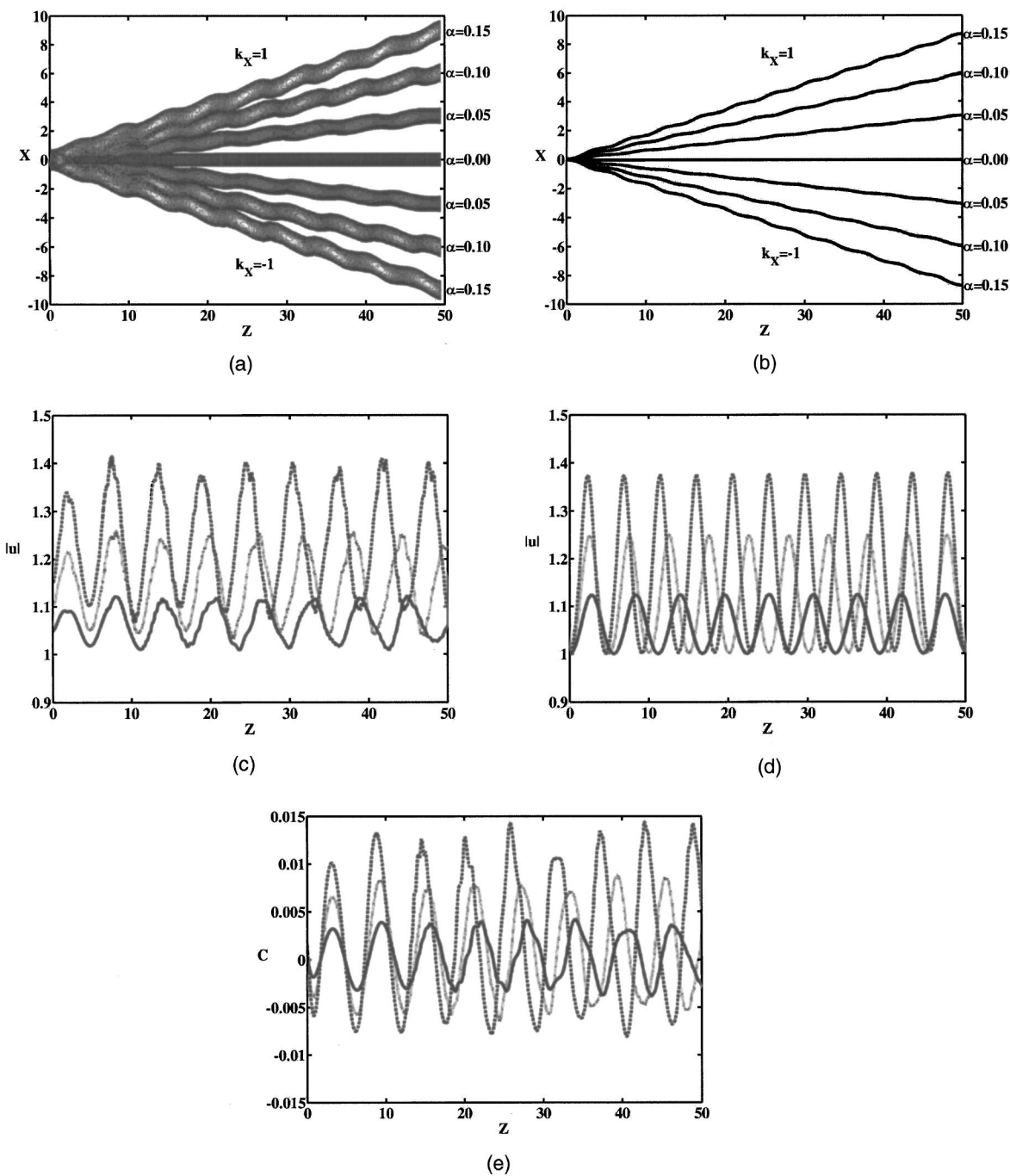


Fig. 2. Interaction of a beam with cw having $k_x = \pm 1$, $\phi = 0$, and $a = 0.05, 0.10$, and 0.15 . (a) Contour plot of beam amplitude as obtained from direct numerical simulation of the NLS equation; (b) beam center X_0 as obtained by numerical integration of the parameter evolution equations; (c), (d) beam amplitude oscillations as obtained from direct numerical simulation of the NLS equation (c) and by numerical integration of the parameter evolution equations (d) for $a = 0.05$ (dark solid curve), $a = 0.10$ (light semi-solid curve), $a = 0.15$ (dotted curve); (e) chirp oscillations as obtained from direct numerical simulation of the NLS equation for $a = 0.05$ (dark solid curve), $a = 0.10$ (light semi-solid curve), and $a = 0.15$ (dotted curve).

chirp, and longitudinal wave number under mixing with a cw. The features of this kind of interactions imply that the intentional launching of a cw having appropriately chosen parameters, namely, amplitude transverse wave number and initial phase, can lead to very promising applications of spatial-soliton control. First, a spatial-soliton input can be dynamically switched between many output ports of an all-optical device if it is mixed with an

appropriate cw. On the other hand, this kind of device can act as a filter that spatially separates beams of different wavelengths, since beams with wave numbers differing significantly from the transverse wave number of the cw pass without changing their velocity, while beams with wave numbers comparable with the cw one deviate to higher angles of propagation. Finally, the strong dependence of the deviation angle on the initial phase differ-

ence with the cw can be utilized in order to detect the phase of a soliton beam and distribute beams of different phase to predefined ports. The results obtained in this work are of a universal nature, since the model used is

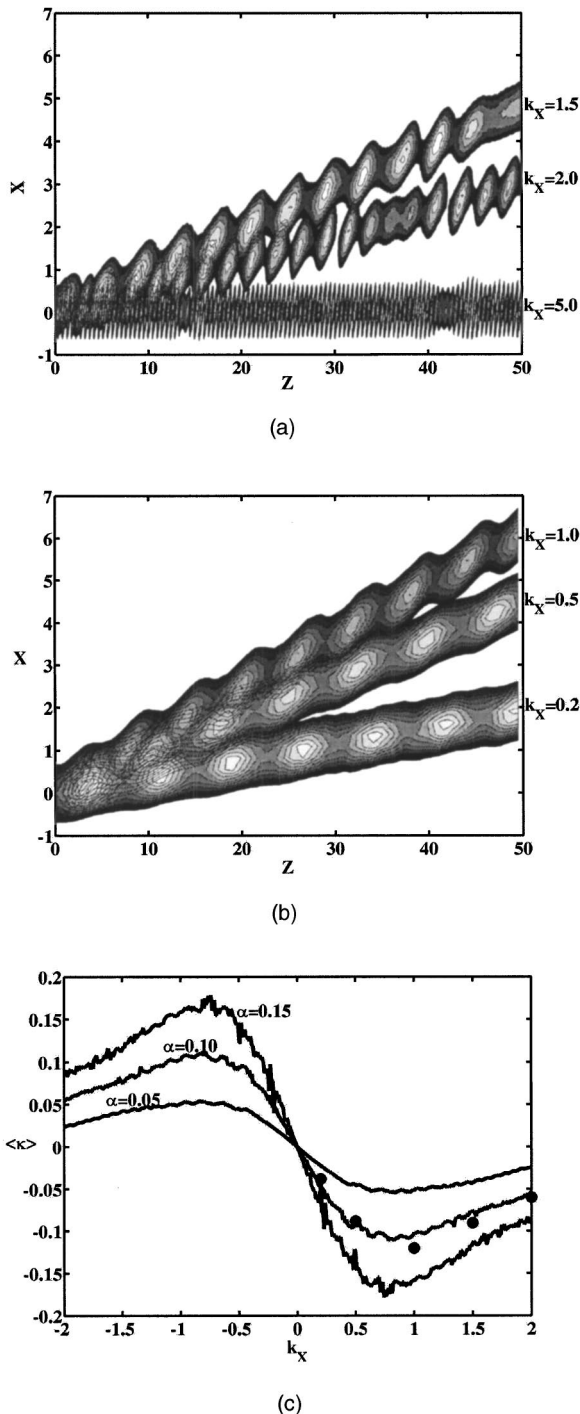


Fig. 3. Beam mean transverse velocity $\langle \kappa \rangle$ versus the cw transverse wave number k_X : (a), (b) Contour plots of the beam amplitude as obtained by direct numerical simulation of the NLS equation for beam interaction with a cw having $\phi = 0$, $a = 0.10$, and $k_X = 0.2, 0.5, 1, 1.5, 2$, and 5 ; (c) $\langle \kappa \rangle$ versus k_X obtained by numerical integration of the parameter evolution equations for $a = 0.05, 0.10$, and 0.15 . For comparison, results from the direct numerical simulations in (a) and (b) are indicated by solid circles.

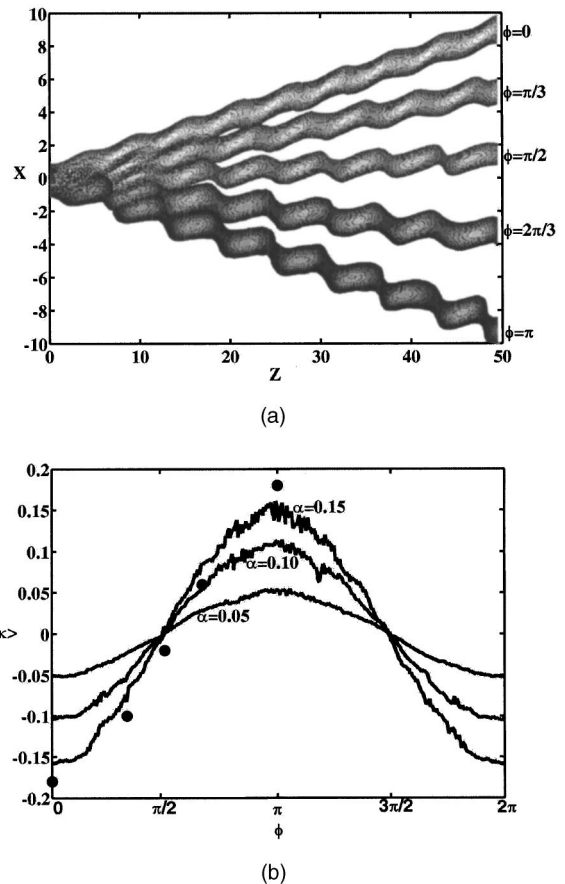


Fig. 4. Beam mean transverse velocity $\langle \kappa \rangle$ versus the initial phase difference ϕ between the cw and the beam: (a) Contour plots of the beam amplitude as obtained by direct numerical simulation of the NLS equation for a beam interacting with a cw having $k_X = 1$, $a = 0.15$, and $\phi = 0, \pi/3, \pi/2, 2\pi/3$, and π ; (b) $\langle \kappa \rangle$ versus ϕ obtained by numerical integration of the parameter evolution equations for $a = 0.05, 0.10$, and 0.15 . For comparison, results from the direct numerical simulations in (a) are indicated by solid circles.

applicable to both spatial and temporal solitons of the NLS equation. Many useful applications, such as frequency control, can also be considered for the temporal soliton case leading to promising optical devices. This is a subject of current and future work.

ACKNOWLEDGMENTS

This research was supported by the "Archimedes" Research Fund of NTUA/ICCS.

REFERENCES

1. J. S. Aitchison, A. M. Weiner, Y. Silberberg, M. K. Oliver, J. L. Jackel, D. E. Leaird, E. M. Vogel, and P. W. E. Smith, "Observation of spatial optical solitons in a nonlinear glass waveguide," *Opt. Lett.* **15**, 471–473 (1990).
2. E. Fazio, M. Zitelli, M. Bertolotti, A. Carrera, N. G. Sanvito, and G. Chiaretti, "Solitonic waveguides in planar glass structures," *Opt. Commun.* **185**, 331–336 (2000).
3. M. Peccianti and G. Assanto, "Signal readdressing by steering of spatial solitons in bulk nematic liquid crystals," *Opt. Lett.* **26**, 1690–1692 (2001).
4. A. Buryak, P. Di Trapani, D. Skryabin, and S. Trillo, "Opti-

- cal solitons due to quadratic nonlinearities: from basic physics to futuristic applications,” *Phys. Rep.* **370**, 63–235 (2002).
5. L. Torner, W. E. Torruellas, G. I. Stegeman, and C. R. Menyuk, “Beamsteering by $\chi^{(2)}$ trapping,” *Opt. Lett.* **20**, 1952–1954 (1995).
 6. A. W. Snyder and D. J. Mitchell, “Spatial solitons of the power-law nonlinearity,” *Opt. Lett.* **18**, 101–103 (1993).
 7. D. N. Christodoulides and M. I. Carvalho, “Bright, dark, and gray spatial solitons states in photorefractive media,” *J. Opt. Soc. Am. B* **12**, 1628–1633 (1995).
 8. A. W. Snyder, D. J. Mitchell, L. Poladian, and F. Ladouceur, “Self-induced optical fibers: spatial solitary waves,” *Opt. Lett.* **16**, 21–23 (1991).
 9. B. Luther-Davies and Y. Xiaoping, “Waveguides and Y-junctions formed in bulk media by using dark spatial solitons,” *Opt. Lett.* **17**, 496–498 (1992).
 10. N. N. Akhmediev and A. Ankiewicz, “Novel soliton states and bifurcation phenomena in nonlinear fibre couplers,” *Phys. Rev. Lett.* **70**, 2395–2398 (1993).
 11. J. J. Rasmussen and K. Ripdal, “Blow-up in nonlinear Schrödinger equation. I. A general review,” *Phys. Scr.* **33**, 481–497 (1986).
 12. A. W. Snyder, A. V. Buryak, and D. J. Mitchell, “Beam splitting on weak illumination,” *Opt. Lett.* **23**, 4–6 (1998).
 13. A. Hasegawa and Y. Kodama, “Amplification and reshaping of optical solitons in a glass fiber. I,” *Opt. Lett.* **7**, 285–287 (1982).
 14. N. N. Akhmediev and S. Wabnitz, “Phase detecting of solitons by mixing with a continuous-wave background in an optical fiber,” *J. Opt. Soc. Am. B* **9**, 236–242 (1992).
 15. R. W. Boyd, *Nonlinear Optics* (Academic, New York, 1992).
 16. J. M. Harbold, F. Ö. Ilday, F. W. Wise, J. S. Sanghera, V. Q. Nguyen, L. B. Shaw, and I. D. Aggarwal, “Highly nonlinear As-S-Se glasses for all-optical switching,” *Opt. Lett.* **27**, 119–121 (2002).
 17. A. Hasegawa and Y. Kodama, *Solitons in Optical Communications* (Clarendon, Oxford, 1995).
 18. J. H. B. Nijhof, W. Forysiak, and N. J. Doran, “The averaging method for finding exactly periodic dispersion-managed solitons,” *IEEE J. Sel. Top. Quantum Electron.* **6**, 330–336 (2000).
 19. R. Scharf and A. R. Bishop, “Length-scale competition for the one-dimensional nonlinear Schrödinger equation with spatially periodic potentials,” *Phys. Rev. E* **47**, 1375–1383 (1993).